Pure & Appl. Chem., Vol. 69, No. 5, pp. 969–978, 1997.
Printed in Great Britain.

Thermodynamic databases and equilibrium calculations in metallurgical processes

Arthur D. Pelton

Centre de Recherche en Calcul Thermochimique
Ecole Polytechnique de Montreal, P. O. Box 6079, Station « Downtown »
Montreal, Quebec, H3C 3A7, CANADA

Abstract : Thermodynamic database computing systems consist of a suite of Gibbs energy minimization programs for the calculation of multiphase multicomponent equilibria coupled with extensive databases for pure substances and multicomponent solutions. The solution databases contain model parameters which are generally obtained by optimization of thermodynamic and phase diagram data of binary and ternary subsystems. The development of large databases is discussed for alloys, slags and glasses, salt solutions, mattes, ceramic solutions, etc. Emphasis is placed upon the proper choice of a model which correctly reflects the structure of the solution. Examples are given of calculations in which these databases are employed to simulate metallurgical and chemical processes such as continuous Pb smelting, ash formation during wood combustion for power generation and refractory corrosion in coal gasification.

INTRODUCTION

In recent years several thermodynamic database computing systems suitable for metallurgical and materials applications have been developed. Three of the largest are F*A*C*T (Montreal), Thermocalc (Stockholm) and MTDATA (Teddington, England). These systems combine databases of the thermodynamic properties of several thousand pure substances and solutions with Gibbs energy minimization software for the calculation of multicomponent multiphase equilibria. The solution data bases contain the parameters of model equations giving the thermodynamic properties as functions of composition and temperature. These parameters are obtained by the critical evaluation and optimization of available data for binary and ternary solutions, and the models are then used to extrapolate to multicomponent solutions.

The aim of the present article is to give a brief introduction to the current state of the art in the thermodynamic modeling of solutions, and to provide a few examples of applications of large evaluated solution databases to the simulation of metallurgical and chemical processes. The examples are taken from the F*A*C*T system of which the author is a co-developer.

A more detailed discussion of the models can be found in references (1, 2).

POLYNOMIAL MODELS

In the simplest model, for a binary solution A-B, the molar Gibbs energy is given by :

$$g = (X_A g_A^O + X_B g_B^O) + RT\,(X_A \ln X_A + X_B \ln X_B) + g^E \qquad (1)$$

where g_i^O is the Gibbs energy of pure i, X_i is the mole fraction of i, and g^E is the excess Gibbs energy which can be expanded as :

$$g^E = \alpha\, X_A X_B = [\,{}^0L + {}^1L(X_B - X_A) + {}^2L(X_B - X_A)^2 + \ldots]\, X_A X_B \qquad (2)$$

where the ${}^iL$ are parameters which are, in general, functions of T. If only the first term, ${}^OL$, is non-zero, then α = *constant* and the solution is « regular ».

A critical evaluation/optimization of a binary solution consists in determining the values of the parameters which best reproduce simultaneously all available data (activities, Gibbs energies, enthalpies of mixing, phase diagrams, etc.) Generally, the experimental phase diagrams is the most useful source of data. Furthermore, since a major practical goal of developing the database is to permit the calculation of heterogeneous equilibria, it is most important to reproduce the phase diagram. As an example, the calculated Pu-U phase diagram (3, 4) is shown in Fig. 1 along with some experimental data points (5-7). Although data points are not shown in the lower part of the diagram, the fit is as good. The optimized parameters used to calculate the diagram are given in Table 1. These were obtained by least-squares optimization of the phase diagram data. Techniques of least squares optimization have been discussed (8-10). The values of g_i^o for the stable phases of Pu and U were taken from the F*A*C*T pure substance database. Note that for a phase such as γ-Pu, in which U is only sparingly soluble, γ_U^o becomes an adjustable model parameter. For the η and ζ phases, both g_{Pu}^o and g_U^o are adjustable model parameters.

Similar optimizations of the U-Zr and Pu-Zr systems have been performed (11,4). Each contains a Γ solid solution phase of the same structure as the Γ(ε-γ) phase in the Pu-U system. To the Gibbs energy of the ternary Γ solution, we apply regular solution theory :

$$g = a_{AB} X_A X_B + a_{BC} X_B X_C + a_{CA} X_C X_A \qquad (2)$$

where A, B, C = U, Pu, Zr. However, we see in Table 1 that α_{PuU} is not constant but is equal to $(730\text{-}390\, X_U)$ in the Pu-U binary system. Similarly α_{PuZr} and α_{UZr} are not constant. For the ternary solution we follow the model of Kohler (12) that α_{ij} = *constant* along lines of constant X_i / X_j ratio. (Other similar models are also used. See (1, 2).) We can now use the model to calculate the solvus surface of the Γ phase in equilibrium with other lower-temperature solids in the ternary system. The resultant calculated solvus is a few degrees lower than the available experimental data, so we add a small adjustable ternary term of $(3800\ X_{Pu} X_U X_{Zr})$ to Eq (2) in order to give the calculated solvus in Fig. 2 (4) which agrees within experimental error limits with all available ternary data.

The binary and ternary parameters are stored in the solution databases. By the systematic optimization of many binary and ternary systems, large multicomponent databases are developed. Eq (2), along with the Kohler or similar models, is used to estimate the properties for a multicomponent solution from the stored parameters of its binary and ternary sub-systems. For example, the Thermocalc system contains extensive databases for ferrous alloys which have been developed in this way.

Such simple polynomial models are based upon regular solution theory which assumes approximately random mixing. Experience has shown that good results are obtained for simple alloys, common-anion or common-cation molten salt solutions and organic liquids (particularly non-polar) in which interactions are relatively weak. For liquids with strong interactions, however, significant short-range ordering occurs, and more sophisticated models must be used.

SHORT-RANGE ORDERING

In the modified quasichemical model (13-15, 1, 2), the exchange of nearest-neighbour pairs in a binary system is considered according to :

$$(A - A) + (B - B) = 2\,(A - B) \qquad (3)$$

The energy for this reaction is $(\omega - \eta T)$. If $(\omega - \eta T)$ is very negative, then (A - B) pairs are favoured. Such is the case, for example, in molten Fe-S solutions. A « quasichemical » equilibrium constant can be written for reaction (3) :

$$K_{AB} = X_{AB}^2 / X_{AA} X_{BB} = 4 \exp[-(\omega - \eta T)/RT] \qquad (4)$$

where X_{ij} is the fraction of total nearest-neighbour pairs which are (i - j) pairs. When $(\omega - \eta T)$ is very negative, the resultant expression for the Gibbs energy of the system goes through a sharp minimum at $X_A = X_B = 0.5$ (1, 2, 13). In order to provide more flexibility in optimizing data, $(\omega - \eta T)$ can be expanded as :

TABLE 1 Optimized Parameters (cal/mol) for the Pu-U System (2)

Liquid	$g^E = X_{Pu} X_U \ (80)$
$\varepsilon - \gamma \ (\Gamma)$	$g^E = X_{Pu} X_U \ (730 - 390 X_U)$
$\delta' - Pu$	$g_U^o = g_U^o(\beta) + (2204 - 0.4745\,T)$
$\delta - Pu$	$g_U^o = g_U^o(\beta) + (2228 - 0.4745\,T)$
$\gamma - Pu$	$g_U^o = g_U^o(\gamma) + (953.5 + 0.8967\,T)$
$\beta - Pu$	$g_U^o = g_U^o(\gamma) + (205.3 + 1.1307\,T)$
$\beta - U$	$g_{Pu}^o = g_{Pu}^o(\varepsilon) + (491.3 + 0.0828\,T)$
$\alpha - U$	$g_{Pu}^o = g_{Pu}^o(\varepsilon) + (-322.0 + 1.792\,T)$
η	$g_{Pu}^o = g_{Pu}^o(\varepsilon) + (-169 + 0.2714\,T)$
	$g_U^o = g_U^o(\beta) + (128 - 0.0838\,T)$
	$g^E = X_{Pu} X_U \ (-760.2 + 1.338\,T - 138.8\,X_U)$
ζ	$g_{Pu}^o = g_{Pu}^o(\varepsilon) + (-669 + 1.7914\,T)$
	$g_U^o = -1742.7 + 31.9883\,T + 4.3500\,(10^{-4})\,T^2$
	$-1.08633\,(10^{-6})\,T^3 - 6.5470\,T\,ln\,T + 11450.0\,T^{-1}$
	$g^E = X_{Pu} X_U \ (-1750 + 200\,X_U)$

$$(\omega - \eta T) = (\omega_o - \eta_o T) + (\omega_1 - \eta_1 T) X_B + (\omega_2 - \eta_2 T) X_B^2 + .. \qquad (5)$$

where ω_i and η_i are the model parameters.

As an example, the activity coefficient of sulphur as measured by several authors in molten Fe-S solutions is plotted in Fig. 3 along with curves calculated from the optimized (16) expression :

$$(\omega - \eta T) = -(70017 + 9\,T) - 74042\,X_S - (798 - 15\,T)\,X_S^3 + 40791\,X_S^7 \quad J/mol \qquad (6)$$

Similar optimizations have been performed (16) for Ni-S and Cu-S solutions. In Cu-S solutions, the sharp Gibbs energy minimum occurs near the composition Cu_2S (33% S). This is accommodated in the model by assuming that $Z_S = 2\,Z_{Cu}$ where Z = coordination number (2, 14, 15). The quasichemical model can now be used to predict the thermodynamic properties of molten Fe-Ni-Cu-S solutions by assuming that the values of K_{ij} in Eq (4) for the quaternary liquid at a sulphur fraction X_S are equal to their values in the binary systems at the same value of X_S. Equilibrium sulphur pressures calculated in this manner (16) with no additional adjustable parameters, are compared with measurements (17) in Fig. 4. In this way, a database for molten Fe-Ni-Cu-Co-Cr-Pb-Zn-S mattes has been developed in the F*A*C*T system (16, 18).

Other models of short-range ordering have been used. For example, Fe-S solutions can be considered to contain FeS associated molecules as well as free Fe and S species. In our experience however, such models, being less physically realistic, yield less satisfactory results.

The quasichemical model for short-range ordering has also been applied with success to other ordered solutions such as ordered liquid alloys. In particular, much success has been achieved in silicate melts and glasses. In a binary silicate, AO_x-SiO_2 (A = Ca, Mg, Na, . . .), the tendency to short-range ordering can be identified with the tendency to form SiO_4^{4-} ions in basic solutions, or with the break-up of the silicate network in acid solutions, and the resultant formation of second-nearest-neighbour (A-Si) pairs. An (Si-Si) pair can be considered to be joined by a doubly-bonded (network) oxygen, an (A-A) pair is a pair of cations separated by an O^{2-} ion, and an (A-Si) pair represents an oxygen bonded to one Si. Hence, the quasichemical reaction (3) is applied for second-nearest-neighbour pairs. This is related to the

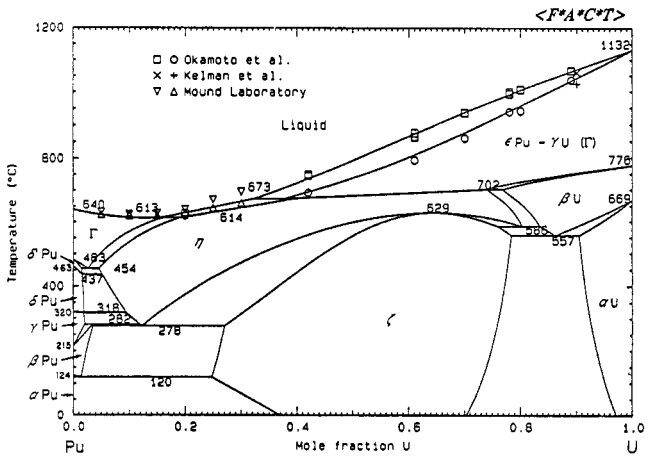

Fig. 1 Calculated optimized Pu-U phase diagram (2)

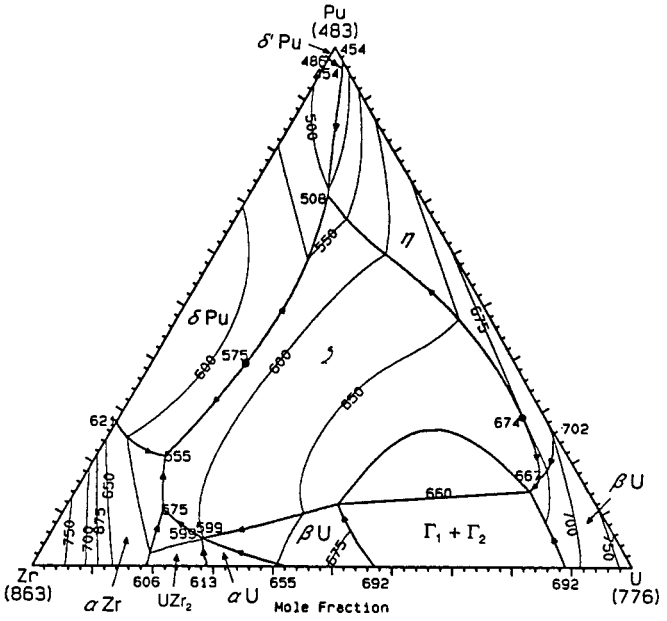

Fig. 2 Calculated projection of the solvus surface of the Γ solid solution phase in the Pu-U-Zr system (4). (T in °C)

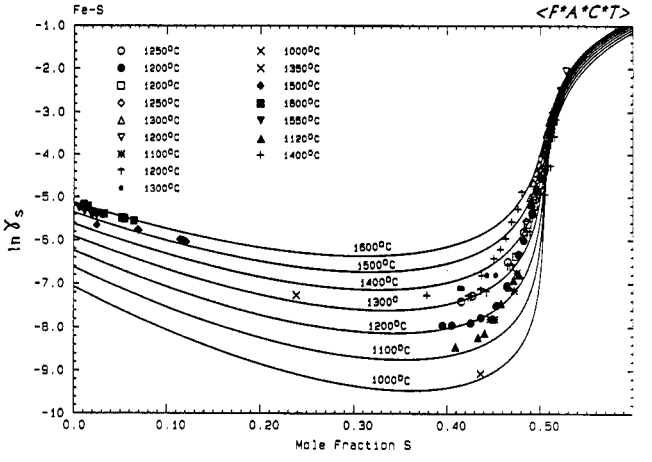

Fig. 3 Activity coefficient of S in liquid Fe-S solutions calculated from optimized model parameters and comparison with experimental data (16)

well-known equilibrium among free, singly-bonded and doubly-bonded oxygen :

$$O^{2-} + O^0 = 2\,O^- \qquad (7)$$

and is also closely related to « cell » models of silicate melts (19).

The quasichemical model has been applied systematically to the optimization of a large number of oxide systems to develop the F*A*C*T slag/glass databases for the oxides of Al, As, B, Ca, Cr(II), Cr (III), Cu(I), Fe(II), Fe(III), Mg, Mn, Na, Ni, Pb, Si, Ti(III), Ti(IV), Zn, Zr. At the same time, optimized databases have been developed for solid oxide solutions (spinels, ilmenites, olivines, perovskites, etc.). An example of an optimized oxide phase diagram is shown in Fig. 5 for the CrO-Cr_2O_3-CaO-SiO_2 system in equilibrium with metallic Cr(20). Agreement with experimental data is within error limits, as is also the case (20) for the system in equilibrium with air. From the optimized database it is then possible to calculate sections at any oxygen pressure as illustrated in Fig. 6.

SUBLATTICE MODELS

The sublattice concept was first developed extensively for molten salt solutions (21). The cations are assumed to form a solution on a cationic sublattice, while the anions form a separate solution on an anionic sublattice. Interactions between ions on the same sublattice are modeled by the excess terms in the common-ion systems (e.g. LiCl-NaCl, NaCl-NaF), while interactions between ions on different sublattices are modeled through the Gibbs energy of exchange reactions, such as :

$$\begin{aligned} &LiCl + NaF = NaCl + LiF \\ &\Delta G = g^{\circ}_{NaCl} + g^{\circ}_{LiF} - g^{\circ}_{NaF} - g^{\circ}_{LiCl} \end{aligned} \qquad (8)$$

For a description of the model for molten salts, see (22). The model has been used to develop an optimized F*A*C*T database for Li, Na, K, Rb, Cs, Mg, Ca/F, Cl, Br, I, OH, NO_3, CO_3, SO_4 and other molten salt solutions as well as for the associated solid solution phases.

The sublattice concept has also proven very successful in modeling the thermodynamics of ceramic phases such as spinels in which the tetrahedral sites constitute one sublattice and the octahedral sites another. Through use of the very useful « Compound Energy Formalism » (23-25), the same mathematical formalism can be used for these solutions as is used for salt solutions. The sublattice model and the Compound Energy Formalism have also been applied, mainly by the Thermocalc group, to the development of extensive databases for interstitial solutions and for intermetallic phases.

SOME APPLICATIONS

A few sample calculations using the solution databases and Gibbs energy minimization software of the F*A*C*T system for metallurgical and materials applications will now be given.

Continuous Pb Smelting

A partial simulation of a continuous Pb smelting process proposed by Noranda/Brunswick Smelting is shown in Figs 7, 8 which are reproduced input/output from the F*A*C*T system. A Pb-Zn-Cu concentrate (also containing Fe, S, As) of the concentration shown in the input at the top of Fig. 7 is mixed with a CaO-SiO_2 flux as shown and is heated with carbon in a counter current of enriched air. The weight ratio of concentrate to air is approximately 1 :1 as simulated in Fig. 7. Data for all possible product phases are automatically retrieved from the databases, and the equilibrium state is calculated by global Gibbs energy minimization. The first (roasting) stage is modeled to occur at 1000°C where reduction by C is very slow. This is simulated by putting 0.0 moles of C in the reactants in Fig. 7. The calculated equilibrium at 1000°C in Fig. 7 shows a slag (oxide) phase rich in Pb and Zn and a matte (sulphide) phase rich in Cu. No metallic phase occurs at this temperature. The formation of an undesirable solid $CaSiO_3$ phase suggests that the flux should be adjusted. At this point the matte phase is removed for separate processing, and the slag phase plus carbon continues to be heated to ~1250°C. In Fig. 8, this second (reduction) stage is modeled by taking as input the slag from the first stage, carbon,

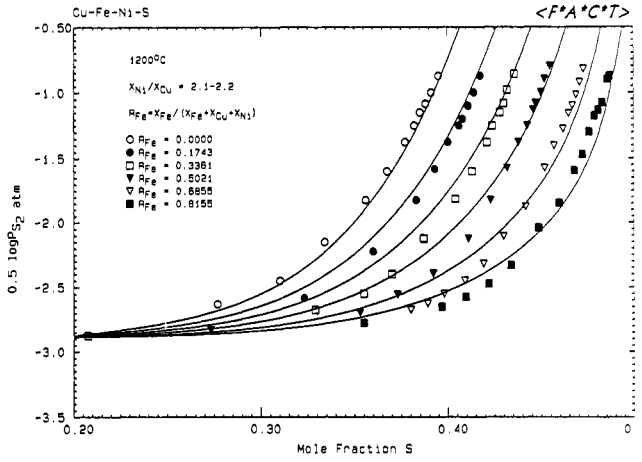

Fig. 4 Equilibrium partial pressure of S_2 at 1200°C over Fe-Ni-Cu-S liquid mattes predicted by the quasichemical model from binary data (16) and comparison with experimental data (17).

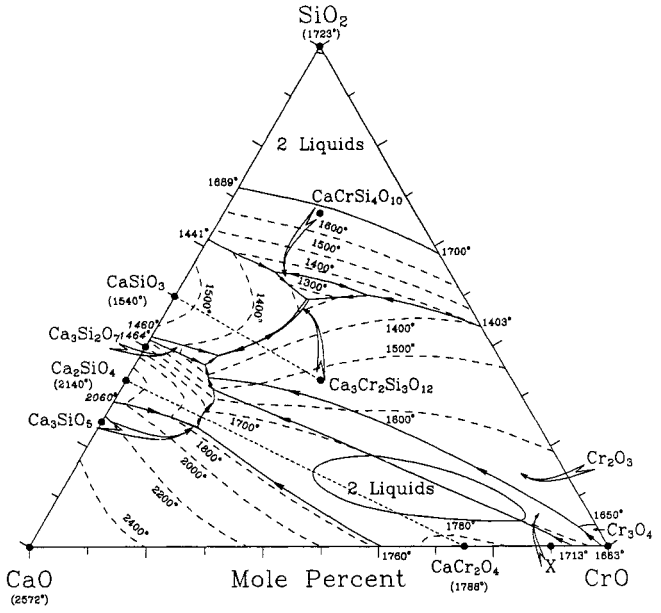

Fig. 5 Calculated (20) projection of the liquidus surface of the Cr-Si-Ca-O in equilibrium with metallic Cr from the Cr corner of the tetrahedron on to the CaO-CrO-SiO_2 plane. (T in °C).

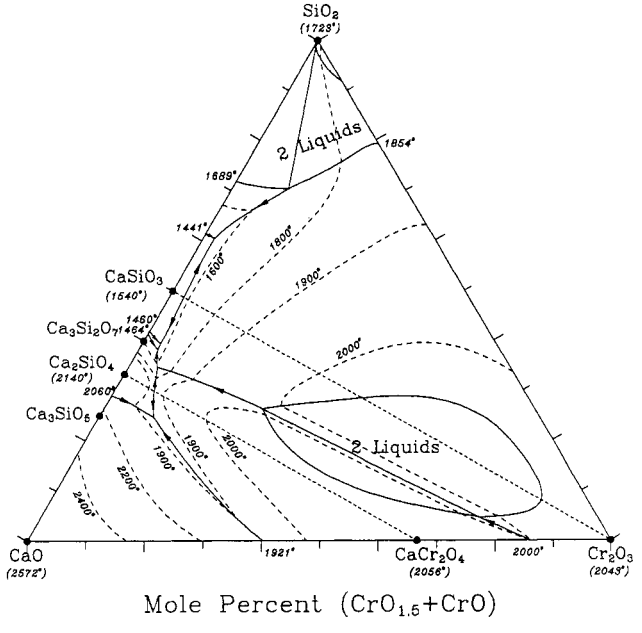

Fig. 6 Calculated (20) projection of the liquidus surface of the Cr-Si-Ca-O system at $p_{O_2} = 10^{-6}$ atm (T in °C).

and some remaining S. At equilibrium an alloy of 97% Pb is achieved, with the Fe remaining in the slag where Pb losses are small. The distribution of As among the gas and other phases is also calculated.

The optimized F*A*C*T databases for the matte and slag phases (quasichemical model) and the molten lead phase (polynomial model) were used. Calculations agree closely with results obtained in laboratory and pilot plant studies (18).

The sulphide content of the slag in Fig. 7 was calculated by a hybrid model (26).

```
(gram) 27.40  Pb + 10.9      Zn + 3.2 Cu + 19.2 Fe +
(gram) 30.00   S +  0.5      As +
(gram) 7.165 CaO + 11.056 SiO2 + 0.0 C  +                    Input
(gram) <0.35A>O2 + <0.65A>N2                  =

A = 118 grammes

    382.11      litre (   74.860      vol% N2
                      +   24.933      vol% SO2
                      +  0.11949      vol% PbS
                      +  0.55204E-01  vol% Pb
                      +  0.24632E-01  vol% PbO              Equilibrium
                      +  0.47054E-02  vol% Zn               gas
                      +  0.18194E-03  vol% S2
                      +  0.10908E-03  vol% As2
                      +  0.17735E-06  vol% O2
                         (1000.00 C, 1.0 atm, Gaz)

+   75.147      gram  (   36.046      wt.% PbO
                      +   22.472      wt.% Fe2O3
                      +   17.958      wt.% ZnO
                      +   12.598      wt.% FeO              Equilibrium
                      +   6.1878      wt.% SiO2             Slag
                      +   1.9824      wt.% Cu2O
                      +   1.5721      wt.% CaO
                      +  0.87187      wt.% As2O3
                      +  0.15108      wt.% PbS
                      +  0.84072E-01  wt.% ZnS
                      +  0.60270E-01  wt.% FeS
                      +  0.86209E-02  wt.% Cu2S
                      +  0.79071E-02  wt.% CaS
                         (1000.00 C, 1.0 atm, Laitier)

+   3.0890      gram  (   60.592      wt.% Cu
                      +   20.902      wt.% Pb
                      +   18.229      wt.% S                Equilibrium
                      +  0.14469      wt.% Zn               Matte (liquid)
                      +  0.10082      wt.% As
                      +  0.31906E-01  wt.% Fe
                         (1000.00 C, 1.0 atm, Matte)

+  0.00000E+00 mol    (  0.28124          Pb
                      +  0.86419E-01      Cu
                      +  0.15953E-01      CuS               Alloy not
                      +  0.15656E-01      S                 formed
                      +  0.26703E-02      As
                      +  0.51994E-05      Zn
                      +  0.58213E-06      Fe
                         (1000.00 C, 1.0 atm, Alliage de Pb, a=0.402)

                      +   12.385      gram CaSiO3                 solid
                         (1000.00 C, 1.0 atm, Sl, a= 1.000 )      formed
```

Fig. 7 Simulation of the first (roasting) stage of the continuous smelting of Pb concentrates (18) near 1000°C with CaO-SiO_2 flux and enriched air

Wood Combustion

The combustion of wood chips over an MgO gravel bed for power production in a turbine is modeled in Fig. 9. The input corresponds to the composition of Aspen wood, which contains appreciable amounts of Si, K, Ca and Al, plus excess air plus the MgO gravel. The process is simulated at 850°C and 4 atm. (27). At equilibrium the ash forms a solid phase rich in K_2SO_4 and also a liquid phase rich in $CaCO_3$ and K_2CO_3 as well as solid CaO, Ca_2SiO_4 and $CaAl_2O_4$. No reaction with the MgO gravel occurs. The F*A*C*T salt databases (sublattice model) were used for the salt phases. The formation of the liquid phase is undesirable because of problems of nozzle blocking, corrosion and turbine fouling. By altering T and P, a window of operation can be found (27) in which no liquid phase forms.

Similar applications to coal combustion and gasification and biomass combustion have proven fruitful in understanding the inorganic chemistry of these processes.

(gram) 23.120 Pb + 10.81 Zn + 0.38 Cu + 19.2 Fe +					
(gram) 1.00 S + 0.45 As +					Input
(gram) 7.165 CaO+ 11.056 SiO_2 + 6.0 C					
(gram) 20.96 O_2 + 0.00 N_2				=	
70.275	litre	(	60.109	vol% CO_2	
		+	28.747	vol% CO	
		+	6.9426	vol% Zn	
		+	2.7550	vol% Pb	
		+	1.0276	vol% PbS	
		+	0.34709	vol% As_2	Equilibrium
		+	0.42144E-01	vol% PbO	gas
		+	0.14160E-01	vol% SO_2	
		+	0.30717E-03	vol% S_2	
		+	0.21220E-07	vol% O_2	
			(1250.00 C, 1.0 atm, Gaz)		
+ 56.035	gram	(	38.110	wt.% FeO	
		+	19.731	wt.% SiO_2	
		+	17.533	wt.% ZnO	
		+	12.240	wt.% CaO	
		+	4.7387	wt.% Fe_2O_3	Equilibrium
		+	3.5415	wt.% PbO	slag
		+	2.0835	wt.% FeS	
		+	0.93806	wt.% ZnS	
		+	0.70354	wt.% CaS	
		+	0.17117	wt.% Cu_2O	
		+	0.16963	wt.% PbS	
		+	0.31627E-01	wt.% As_2O_3	
		+	0.85069E-02	wt.% Cu_2S	
			(1250.00 C, 1.0 atm, Laitier)		
+ 0.00000E+00 mol		(	0.42724	Pb	
		+	0.15298	S	Matte not
		+	0.11476	Cu	formed
		+	0.60415E-01	Zn	
		+	0.45010E-02	Fe	
		+	0.28972E-03	As	
			(1250.00 C, 1.0 atm, Matte, a=0.760)		
+ 17.203	gram	(	97.292	wt.% Pb	
		+	1.6002	wt.% Cu	
		+	0.80021	wt.% As	Equilibrium
		+	0.13675	wt.% CuS	alloy (liquid)
		+	0.88265E-01	wt.% S	
		+	0.71844E-01	wt.% Zn	
		+	0.10421E-01	wt.% Fe	
			(1250.00 C, 1.0 atm, Alliage de Pb)		

Fig. 8 Simulation (18) of the second (reduction) stage of the slag from Fig. 7 near 1250°C with carbon after the matte has been removed.

Refractory Corrosion in Coal Gasification

As a final example, a study was performed for the Alberta Research Council of the degradation of Cr_2O_3-Al_2O_3 refractories in the presence of coal gasification slags. Results are shown in Fig. 10 for a slag of composition (wt %) (45 SiO_2, 25 Al_2O_3, 19 CaO, 4 Fe_2O_3, 7 Na_2O) at 1400°C in the presence of a gas with P_{O_2} = 5 x 10^{-10} bar (28). The process was studied by simulating the dissolution of progressively larger amounts of Cr_2O_3 and Al_2O_3 in the weight ratio 70 :26 which is found in the refractory. After bout 0.2 g of Cr_2O_3 per 100 g. slag is dissolved, equilibrium with the precipitating corundum (Cr_2O_3-Al_2O_3) solid solution is achieved. Degradation will nevertheless continue, albeit slowly, because the equilibrium Cr_2O_3 content of the solution is less than that of the refractory. When about 0.7 g of Cr_2O_3 have eroded, the dissolved Cr_2O_3 and Al_2O_3 begin to react partially with the Fe in the slag to precipitate spinel with a resultant probable increase in the erosion rate. The degradation was studied by simulation with different gas compositions (which affect the Fe^{2+}/Fe^{3+} ratio in the slag and thus influence the process) as well as with different slags, refractories and temperatures. The sublattice model was used for the (Fe, Cr, Al) spinel phase.

```
(gram) 51.57 C + 6.24 H + 617.88 N + 0.02 S +
(gram) 226.96 O + 0.00079 Si + 0.0810 K + 0.15242 Ca +      Input
(gram) 0.00101 Al + 500 MgO   =

    30.693      mol   (  0.71859          N2
                    +  0.13987          CO2
                    +  0.10085          H2O
                    +  0.40635E-01      O2              Equilibrium
                    +  0.48782E-04      NO              gas
                    +  0.96606E-05      KOH
                    +  0.10515E-05      NO2)
                       (850.0 C, 4.0 atm, gas)

+  0.53788E-03 mol   (  0.54809          CaCO3
                    +  0.40732          K2CO3
                    +  0.25580E-01      CaSO4           Liquid carbonate
                    +  0.19010E-01      K2SO4)          formed
                       (850.0 C, 4.0 atm, liquid)

+  0.65805E-03 mol   (  0.90964          K2SO4
                    +  0.89464E-01      K2CO3
                    +  0.81712E-03      CaSO4           Solid sulphate
                    +  0.80365E-04      CaCO3)          formed
                       (850.0 C, 4.0 atm, solid)

                    +   12.406      mol  MgO
                    +  0.34188E-02  mol  CaO             Other solid phases
                    +  0.28128E-04  mol  Ca2SiO4         at equilibrium
                    +  0.18716E-04  mol  CaAl2O4
```

Fig. 9 Simulation of the combustion of Aspen wood in air at 850°C and 4 atm for power production (27)

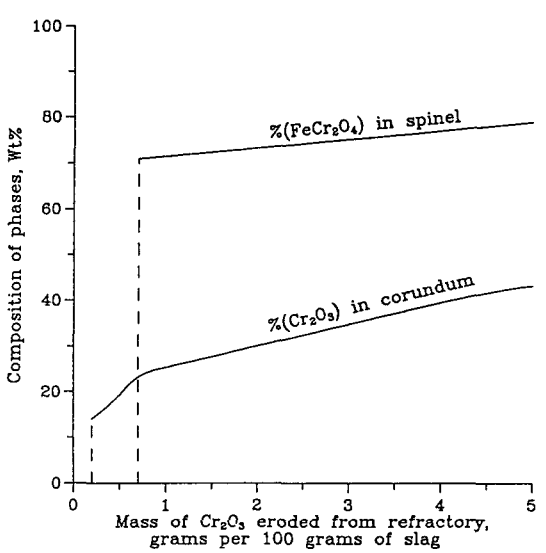

Fig. 10 Precipitation of solid phases from coal gasification slag resulting from the dissolution of Cr_2O_3-Al_2O_3 refractory at 1400°C

REFERENCES

1. A.D. Pelton, Ch. 1 in *Materials Science and Technology*, **vol. 5** (R.W. Cahn, P. Haasen and E. J. Kramer ed.), pp 1-75, VCH, NY (1991).
2. A.D. Pelton, Ch. 3 in *Advanced Physical Chemistry in Process Metallurgy* (N-Sano, W.-K. Lu, P.V. Riboud and M. Maeda ed.) Academic, NY, in press.
3. L. Leibowitz, R.A. Blomquist and A.D. Pelton, *J. Nucl. Mater.*, **167**, 76-81 (1989).
4. P.K. Talley, A.D. Pelton and L. Leibowitz, to be submitted to *J. Nucl. Mater.*
5. F. H. Ellinger, R.O. Elliott and E.M. Cramer, *J. Nucl. Mater*, **3**, 233, (1959).
6. L.R. Kelman, H. Savage, C.M. Walter, B. Blumenthal, R.J. Dunworth and H.V. Rhude, in *Plutonium 1965*, (A.E. Kay and M.B. Wadron ed.) pp. 458-484, Chapman and Hall, London (1967).
7. Mound Laboratory Report MLM-1402, Miamisburg, Ohio (1967).
8. H.L. Lukas, E.-Th. Henig and B. Zimmermann, *Calphad*, **1**, 225-236 (1977).
9. P. Dörner, E.-Th. Henig, H. Krieg, H.L. Lukas and G. Petzow, *Calphad*, 4, 241-254 (1980).
10. C.W. Bale and A.D. Pelton, *Metall. Trans.*, **14B**, 77-84 (1983).
11. L. Leibowitz, R.A. Blomquist and A.D. Pelton, *J. Nucl. Mater.*, 184, 59-64 (1991).
12. F. Kohler, *Monatsh. Chem.*, 91, 738 (1960).
13. A.D. Pelton and M. Blander, *Proc. AIME Sympos. Molten Salts and Slags*, pp. 281-294, Am. Inst. Met. Eng., Warrendale, PA (1984).
14. A.D. Pelton and M. Blander, *Metall. Trans.*, 17B, 806-815 (1986).
15. M. Blander and A.D. Pelton, *Geochim. Cosmochim. Acta*, 51, 85-95 (1987).
16. F. Kongoli, M. Sc. App. Thesis, École Polytechnique, Montréal (1996).
17. C.W. Bale and J. Toguri, private communication (1996).
18. Y. Dessureault, Ph.D. thesis, École Polytechnique (1993).
19. M.L. Kapoor and M.G. Frohberg, *Sympos. Chem. Metall. Iron and Steel*, Sheffield, England (1971).
20. S. Degterov and A.D. Pelton, *Metall. Trans.*, submitted
21. M. Blander, Ch.3 in *Molten Salt Chemistry* (M. Blander, ed.), Interscience, NY (1964).
22. A.D. Pelton, *Calphad*, 12, 127-142 (1988).
23. B. Sundman and J.Ågren, *J. Phys. Chem. Solids*, 42, 297 (1981).
24. M. Hillert, B. Jansson and B. Sundman, *Z. Metallk.*, 79, 81 (1988).
25. T. I. Barry, A.T. Dinsdale, J.A. Gisby, B. Hallstedt, M. Hillert, B. Jansson, J. Jonsson, B. Sundman and J.R. Taylor, *J. Phase Equil.*, 13, 459-476 (1992).
26. A.D. Pelton, G. Eriksson and A. Romero-Serrano, *Metall. Trans.*, 24B, 817-825 (1993).
27. M. Blander, KW. Ragland, R.L. Cole, J.A. Libera and A.D. Pelton, *Biomass and Bioenergy*, 8, 29-38 (1995).
28. S. Degterov and A.D. Pelton, *Proc. Am. Ceram. Soc. Symposium*, in press.